EXTENDED X-RAY EMISSIONS FROM THE RADIO GALAXY CENTAURUS B

M. Tashiro
Saitama University
Sakura, Saitama, 338-8570, Japan
TASHIRO@PHY.SAITAMA-U.AC.JP
N. Isobe, M. Suzuki, K. Ito, K. Abe, K. Makishima
ISOBE.NAOKI@JAXA.JP, SUZUKI@HEAL.PHY.SAITAMA-U.AC.JP, KITO@HEAL.PHY.SAITAMA-U.AC.JP
ABE@HEAL.PHY.SAITAMA-U.AC.JP, MAXIMA@PHYS.S.U-TOKYO.AC.JP

Abstract

Inverse-Compton X-rays from radio lobes and jets were long expected to determine the energy of electrons and magnetic field in radio lobes without assuming energy equipartition. In 1998, the radio galaxy Centaurus B became the first object that exhibited non-equipartition in the radio lobes (Tashiro et al. 1998). That result suggested a structure caused by possible energy transportation from particles to the magnetic fields in outflows, and large scale structures have been suggested by some authors (e.g., Isobe et al. (2002)). We present an *XMM-Newton* observation which reveals middle scale X-ray structures, associating a jet and an inner lobe. With the fine spatial resolution, we resolve jet-like structures, from which cosmic microwave background boosted inverse-Compton X-rays are radiated, and derive physical quantities of magnetic field and electron energy.

1 Introduction

Discovery of inverse-Compton (IC) X-rays in radio lobes which are produced from cosmic microwave background (CMB) photons provided us with a reliable method to investigate long discussed jet-lobe energetics (Kaneda et al., 1995; Feigelson et al., 1995). The method was long proposed to determine the magnetic field and electron energy densities by measuring the ratio of synchrotron radio to IC X-ray flux (e.g., Harris & Grindlay (1979)). This method is free from the minimum energy assumption, so that it is possible to show non-equipartition states in radio lobes. It is hence expected to provide a reliable way to investigate relative dominance between particles and fields in the outflows from the active galactic nucleus (AGN). With *ASCA*, Tashiro et al. (1998) firstly obtained evidence of deviation from particle-field equipartition in the radio galaxy Centaurus B (McAdam (1991): PKS $1343-601$; z = 0.01215; West & Tarenghi (1989)), in which they concluded electron energy domination against that of the magnetic field. In addition, they reported a significant displacement of the brightness peaks in radio and X-ray bands. The obtained inner brightened X-ray emission suggests energy transportation from electrons to magnetic fields along the lobes, although they were not able to investigate in detail due to the limited imaging capability of *ASCA*.

In this contribution, we present results from an *XMM-Newton* observation of the double lobe radio galaxy Centaurus B. The radio galaxy is the second brightest extragalactic radio source in the GHz band in the southern sky (McAdam 1991 and references therein). McAdam (1991) used the high resolution 843 MHz interferometer MOST to show that its nucleus is linked by a dual jet to asymmetric lobes surrounded by a confined low-brightness balloon ($270\times130h_{75}^{-2}$ kpc^2). The relatively large size and the high radio brightness make the lobes an ideal target of an IC X-ray study with the good sensitivity and imaging capability of *XMM-Newton*.

2 Observation and results

We carried out the *XMM-Newton* observations of Centaurus B, as part of the Guest Observer Cycle 1 phase, on 25 August, 2001. We operated the EPIC-MOS 1, 2 and pn cameras in the Prime Full Window mode. The

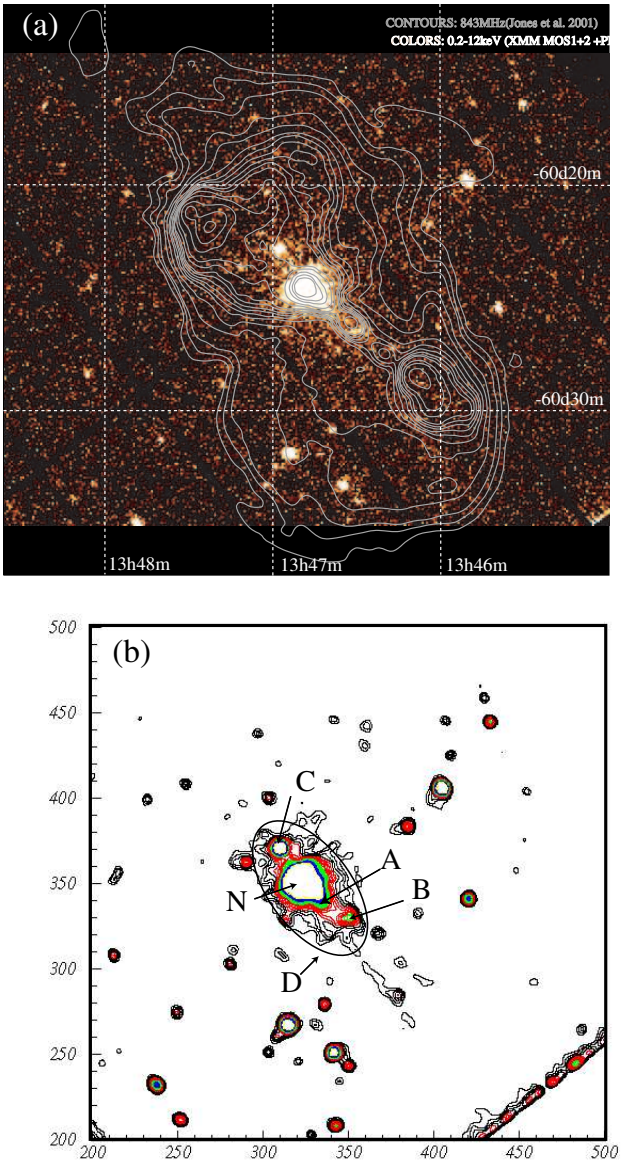

Figure 1: (a) The 0.3–7 keV background-inclusive EPIC image of Centaurus B, is binned into 4×4 pixels. A VLA radio image obtained by Jones et al. is overlaid as contours (Jones et al., 2001). (b) Smoothed contour map of the X-ray image: point sources N and C and diffuse emissions A, B and D are labeled (see text).

duration of the observation was 32 ks and we obtained 28 ks of good time after the standard data reduction process.

2.1 X-ray image

In Fig. 1(a), we show a background-inclusive 0.7–7 keV raw EPIC+pn image of the source, binned into 4×4 EPIC pixels, and a radio image obtained by Jones et al. (2001) in contours. We saw a bright X-ray source at the nucleus and a significant elongation toward the south-west from the galaxy. We also saw a point like source in the north-east of the galaxy. In Fig. 1(b), we show a smoothed profile of X-ray brightness map in contours. We confirmed a significant one side elongation (A) in the south-west direction and a plug like structure (B) at the end. Since we saw no significant elongation on the other side of the nucleus, the extension could not to be due to artificial structure, e.g., due to the point spread function of the mirror. The source (B) spatially coincides with a stellar object USNO 0225−18993558 within the accuracy. It is, however, not likely to be attributed to the stellar object, because of the extended shape in the X-ray (Fig. 2). On the other hand, we found coincidence of the north-east point-like source (C) with a stellar object USNO 0225−18016269 within the position accuracy. The source (C) is also seen in infra-red bands in which we saw the source exhibiting a color consistent with a normal star.

In addition to these discrete structures, we saw significant diffuse emission elongated along the radio jet direction and extended over the source (B). In order to examine the extended emission, we present a projected profile along the jet directions (black) in Fig. 2, in which we also show a profile perpendicular to the jet axis in gray. The obtained profile along the jets shows two prominent point sources in the central nucleus and at the position of the stellar object (C), and confirms the significant excess emission along the south-west jet over the sources (A) and (B).

To conclude, we detected X-ray emission from the nucleus (N), south-west X-ray jet (A) and its plug like feature (B), and surrounding diffuse emission elongated along the jet axis. In addition to these emissions from the radio galaxy there was a contaminant foreground stellar object (C) north-east of the nucleus.

2.2 X-ray spectra of the features

In order to study the X-ray emission mechanism from the observed structures, we evaluated the EPIC and pn spectra from the sources (N), (A), (B) and (C) independently. Then we examined the EPIC and pn spectra from the oval region (D) (Fig. 1) to evaluate the diffuse emission.

The nucleus exhibits non-thermal X-ray emission with intrinsic absorption, whose energy index and

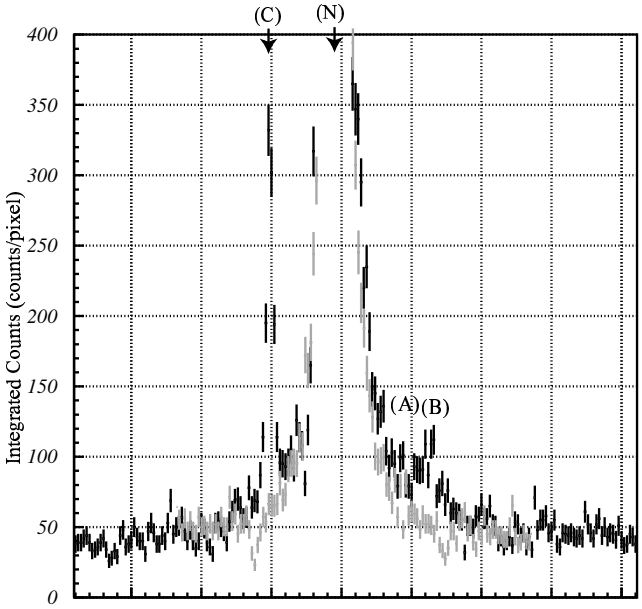

Figure 2: The 0.3–7 keV background-inclusive projection profile of Centaurus B. Projection along the jets is indicated in black, while perpendicular to the jets is indicated in gray. The profile is shown from north-east to south-west. Two point-like sources (N), (C) and significant diffuse emission (A), (B) and outside of (B) along the south-west jet are seen.

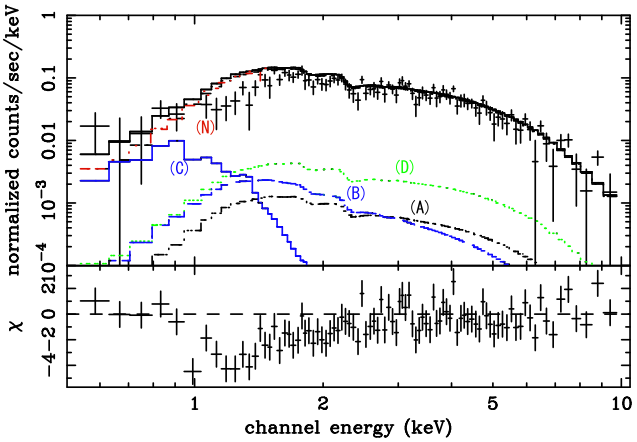

Figure 3: EPIC background subtracted spectrum from the region (D). X-ray spectral components evaluated for region (N), (A), (B), and (C) are indicated to describe the discrete emissions.

photo-absorption column density are 0.56±0.02 and 1.7×10^{26} m^{-2}. The derived 2–10 keV flux density of 5.4×10^{-15} W m^{-2} corresponds to a 2–10 keV rest frame luminosity of 1.5×10^{35} W. The obtained spectral parameters are all consistent with those expected for a typical radio galaxy nucleus, although we see a significant decrease of the active nucleus luminosity in comparison with that measured by Tashiro et al. (1998).

From the source (A), associated with the south-west radio jet, we obtained an hard X-ray spectrum, with a spectral energy index of 0.43±0.17, and the derived luminosity from source (A) is 5.6×10^{33} W. The diffuse source (B) placed at the end of the source (A) structure has an X-ray flux 21% that of source A, while the X-ray spectrum exhibits a consistent slope whose energy index of 0.66±0.43 is consistent with that of (A).

In contrast to these diffuse emissions, we see that source (C) exhibits a much softer spectrum. Although the X-ray flux is fainter even than that from source (B), we described the X-ray spectrum with a soft power-law model and used a thermal plasma emission model to evaluate the flux. The derived energy index and temperature, 1.6±0.3 and 0.14 keV, respectively, are consistent with that expected from a stellar object.

Finally we evaluated the residual diffuse component (D). Since the region (D) includes the structures (N), (A), (B), and (C), we employed the best-fit spectra obtained above to describe the discrete components, then we introduced an additional power-law component to evaluate the residual diffuse hard X-ray emission. The derived energy index of 0.4±0.3 is too hard to be attributed to galactic halo plasmas but consistent with those obtained from nucleus and jet component. Beside the nucleus emission, the fractions of X-ray fluxes from the structures are 71%, 21%, 5%, and 3% from the features (D), (A), (B), and (C), respectively, and the total flux is consistent with that measured by *ASCA* as diffuse emission (Tashiro et al. (1998)).

3 Discussion

We observed a hard X-ray emission from the one-side X-ray jet labeled A. The obtained X-ray spectrum is well described with a power-law function modified with the Galactic absorption. The best fit spectral index of α = 0.4±0.3 exhibits consistent or flatter spectral slope in comparison with that obtained from a 4.80 GHz observation of the same region ($\sim$ 1–1.5) (Jones et al., 2001). In addition to that, the measured X-ray flux density exceeds that of radio by an order of magnitude, which implies that IC is the dominant process producing the X-rays.

Jones et al. (2001) showed that the radio emission from the south jet exceeds that from the north jet by a factor

Table 1: Derived physical quantities of extended structures

X-ray feature	$u_{\rm e}$ (J m^{-3})	$u_{\rm m}$ (J m^{-3})
A	$(6\times10^{-10})\Gamma^6$	$(4\times10^{-17})\Gamma^2$
B	$(3\times10^{-13})\Gamma^6$	$(5\times10^{-16})\Gamma^2$
D	6×10^{-13}	7×10^{-15}

of 2.5. Assuming the discrepancy comes from the relativistic beaming effect, we estimated the relativistic boosting effect from the jet-counter-jet ratio $R = 2.5 = \left(\frac{1+\beta\cos\theta}{1-\beta\cos\theta}\right)^{2+\alpha}$. If we take the spectral index $\alpha = 1.0$, according to Jones et al. (2001), we obtain $\beta\cos\theta = 0.15$, and $\delta \sim 30\Gamma^{-1}$. Adopting the estimated Doppler factor (δ), we evaluated the seed photon densities from four candidate sources; (1) synchrotron radio emission from the jet, (2) nucleus, (3) stellar emission from the galaxy, and (4) the CMB, according to Stawarz, Sikora & Ostrowski (2003), and found that the CMB is the dominant seed photon source.

As for the diffuse emission (D) from the inner lobe region, the obtained brightness profile suggests a homogeneous emissivity of a spheroidal volume. We naturally assume that the emission region is non-relativistic in motion, considering the large and homogeneous morphology. Since the source (D) X-ray luminosity exceeds the extrapolation of the radio luminosity from the same region, IC is thought to be the emission process. Assuming an axisymmetric emission volume, the CMB is the dominant source of the IC X-rays.

Thus we derived the physical quantities as summarized in Table 1, assuming the electron energy range to be $\gamma = 10^{3-6}$. Although the derived quantities still depend on the Lorentz factor (Γ), we see that the electron energy density overwhelms that of the magnetic field in every structure. Assuming a bulk Lorentz factor (Γ) of a few, the derived magnetic field energy densities range from 10^{-15} J m^{-3} to 10^{-16} J m^{-3}. On the other hand, $u_{\rm e}$ dissipates 10^{-7}–10^{-13} along the jet-lobe outflow.

The result supports significant particle dominance against the magnetic fields in jets and inner lobe regions as reported by authors (e.g., Brunetti et al. (1999); Brunetti et al. (2002); Hardcastle et al. (1998); Hardcastle & Worall (1999); Hardcastle et al. (2002); Grandi et al. (2003); Tashiro et al. (1998) and in summary Isobe et al. (2005) in this issue) , and also suggest that energy dissipation from jet to lobe is mainly due to particles. These trends were also suggested by authors including Tashiro et al. (1998), Tashiro et al. (2001), Jones et al. (2001), and Isobe et al. (2002).

Acknowledgments

We appreciate the organizers and participants of the conference for fruitful discussions at the meeting.

References

Brunetti, G., Comastri, A., Setti, G., Feretti, L. 1999, A&A, 342, 57

Brunetti, G., Bondi, M., Comastri, A., Setti, G. 2002, A&A, 381, 795

Feigelson, E. D., Laurent-Muehleisen, S. A., Kollgaard, R. I., Fomalont, E. B. 1995, ApJ, 449, L149

Grandi, P., Guainazzi, M., Maraschi, L., Morganti, R., Fusco-Femiano, R., Fiocchi, M., Ballo, L., Tavecchio, F. 2003, ApJ, 586, 123

Harris, D. E., Grindlay, J. E. 1979, MNRAS, 188, 25

Hardcastle, M. J., Alexander, P., Pooley, G. G., Riley, J. M. 1998, MNRAS, 296, 445

Hardcastle, M. J., Worall, D. M. 1999, MNRAS, 309, 969

Hardcastle, M. J., Birkinshaw, M., Cameron, R. A., Harris, D. E., Looney, L. W., Worall, D. M. 2002, ApJ, 581, 948

Isobe, N., Tashiro, M., Makishima, K., Iyomoto, N., Suzuki, M., Murakami, M., Mori, M. Abe, K. 2002, ApJ, 581, L111

Isobe, N., Tashiro, M., Makishima, K., Iyomoto, N., Kaneda, H., Suzuki, M., Abe, K., Mori, M. 2005, *"X-Ray and Radio Connections"* eds. Sjouwerman, L. O. & Dyer, K. K., Published electronically at http://www.aoc.nrao.edu/events/xraydio

Jones, P. A., Lloyd, B. D., McAdam, W. B. 2001, MNRAS, 325, 817

Kaneda, H., Tashiro, M., Ikebe, Y., Ishisaki, Y., Kubo, H., Makshima, K., Ohashi, T., Saito, Y., Tabara, H., Takahashi, T. 1995, ApJ, 453, L13

McAdam, W. B. 1991, Proc. Astron. Soc. Aust., 9, 255

Stawarz, Ł., Sikora, M., Ostrowski, M. 2003, ApJ, 597, 186

Tashiro, M., Kaneda, H., Makishima, K., Iyomoto, N., Idesawa, E., Ishisaki, Y., Kotani, T., Takahashi, T., Yamashita, A. 1998, ApJ, 499, 713

Tashiro, M., Makishima, K., Iyomoto, N., Isobe, N., Kaneda, H. 2001, ApJ, 546, L19

West, R. M., Tarenghi, M. 1989, A&A, 223,61